Nanoscale

Accepted Manuscript

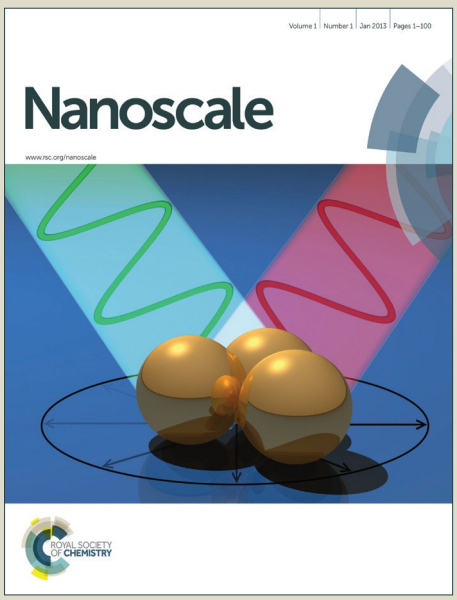

ROYAL SOCIETY OF CHEMISTRY

www.rsc.org/nanoscale

Nanoscale

PAPER

Nitrogen-doped carbon nanoparticles modulated turn-on fluorescence probes for histidine detection and its imaging in living cells

Received 00th January 20xx,
Accepted 00th January 20xx

DOI: 10.1039/x0xx00000x

www.rsc.org/

Xiaohua Zhu,[a b] Tingbi Zhao,[b] Zhou Nie,*[a] Zhuang Miao,[c] Yang Liu*[b] Shouzhuo Yao[a]

In this work, nitrogen-doped carbon nanoparticles (N-CNPs) modulated turn-on fluorescence probes were developed for rapid and selective detection of histidine. The as synthesized N-CNPs exhibited high fluorescence quantum yield and excellent biocompatibility. The fluorescence of N-CNPs can be quenched selectively by Cu (II) ions with high efficiency, and restored by the addition of histidine owing to the competitive bind of Cu (II) ions and histidine that removes Cu(II) ions from the surface of the N-CNPs. Under the optimal conditions, a linear relationship between the increased fluorescence intensity of N-CNPs/Cu (II) ions conjugates and the concentration of histidine was established in the range from 0.5 to 60 μM. The detection limit was as low as 150 nM (signal-to-noise ratio of 3). In addition, the as prepared N-CNPs/Cu(II) ions nanoprobes showed excellent biocompatibility and were applied for histidine imaging assay in living cells, which presented great potential in the bio-labeling assay and clinic diagnostic applications.

1. Introduction

Histidine, an essential amino acid in humans and other mammals, plays crucial roles in a number of proteins for growth and repair of tissues. Furthermore, it controls the transmission of metal elements in biological bases and acts as neurotransmitter or neuromodulator in the central nervous system of mammals.[1-3] The abnormal expression level of histidine has been considered as an indicator for many diseases. For example, the low level of histidine in blood plasma may induce rheumatoid arthritis, nerve deafness, liver cirrhosis and pulmonary disease.[4, 5] While, the overexpression of histidine is associated with several diseases, such as cancer, AIDS, Alzheimer's disease, and chronic kidney disease.[6, 7] As a result, rapid and sensitive assessment of histidine expression in blood plasma and intracellular is essential in clinic diagnostic and help to understand the pathogenesis for clinical therapy.

Several methods have been developed for the determination of histidine, including liquid chromatography,[8] capillary electrophoresis,[9] electrochemistry,[10, 11] colorimetry,[12, 13] and fluorescent spectrometry.[14, 15] Compared with other techniques, the fluorescence method exhibits more advantages such as the operational simplicity, high-throughput process, real-time detection and good sensitivity and selectivity.[16-19] Up to now, a large number of fluorescent probes, such as DNA and organic molecule have been developed for fluorescence detection of histidine.[20-22] For example, based on the highly specific interaction between the amino acids and the metal ions and the strong fluorescence thiazole orange/DNA probe in a competition assay format, a fluorescence turn-on assay for detection of histidine was developed.[22] A Cu^{2+} coupled naphthalimide complex was used as a turn-on fluorescent probe for the detection of histidine in aqueous solution and living cells.[23] In the past decade, nanomaterials have gained increasing interest due to their unique and novel properties.[24-27] Some novel and efficient nanomaterial-based fluorescence probes, such as fluorescent semiconductor quantum dots (QDs) and metal nanoclusters have been developed.[24, 25, 28-35] For instance, a tyrosine-functionalized $CuInS_2$ QDs was employed for the determination of biothiols, histidine and threonine.[29] The Ag/Au bimetallic nanoclusters was exploited as an integrated logic gate and a specific fluorescence turn-on assay for selectively and sensitively sensing histidine and cysteine.[36] However, the potential toxicity and environment hazards due to the heavy metals essential elements in these conventional nanomaterials cause new concerns. The environmental benign nanomaterials with excellent fluorescence properties are desired.

Owing to the distinct advantages of biocompatibility, low toxicity and photostability, fluorescent carbon nanoparticles

[a] State Key Laboratory of Chemo/Biosensing and Chemometrics, College of Chemistry and Chemical Engineering, Hunan University, Changsha 410082, People's Republic of China. E-mail: niezhou.hnu@gmail.com; Fax: +86-731-88821848; Tel: +86-731-88821626
[b] Department of Chemistry, Beijing Key Laboratory for Analytical Methods and Instrumentation, Key Lab of Bioorganic Phosphorus Chemistry and Chemical Biology of Ministry of Education, Tsinghua University, Beijing 100084, China. E-mail: liu-yang@mail.tsinghua.edu.cn. Tel: 86-10-62798187. Fax: 86-10-62771149.
[c] Departments of Neurosurgery, China-Japan Union Hospital of Jilin University, Changchun, Jilin 130033, China.

Electronic Supplementary Information (ESI) available: [details of any supplementary information available should be included here]. See DOI: 10.1039/x0xx00000x

(CNPs) have drawn much attention in the past decade.[19, 37-41] CNPs have been used as high efficient fluorescence probes for metal ions,[42, 43] small biomolecules,[44, 45] and proteins detection and *in vivo* imaging.[46-48] CNPs are more superior to traditional organic dyes and semiconductor quantum dots in terms of aqueous solubility, biocompatibility, and easy functionality, which make them fascinating in biosensing and imaging applications.[49, 50] Recently, a histidine fluorescence sensor has been developed based on the recovered fluorescence of the carbon quantum dots (CQDs)-Hg (II) ions system.[51] Though the fluorescence exhibited high sensitivity and rapid operation, the toxicity of Hg (II) ions and limited fluorescence quantum yield of the CQDs limited its biomedical applications. It is still a challenge to the synthesis of biocompatible and highly fluorescent water-soluble CNPs in the bioassay and intracellular imaging applications. Nitrogen doping is an effect way to improve the fluorescence quantum yield of CNPs,[52, 53] and we have shown that nitrogen doped carbon nanoparticles can be synthesized by a green and facial solid phase method with very high fluorescence quantum yield, which are quite suitable to the biomedical assay.[54]

Herein, a nitrogen-doped carbon nanoparticles coupled Cu (II) ions (N-CNPs/Cu(II) ions) complex was developed as a turn-on fluorescence probe for histidine detection. The N-CNPs were synthesized by a green and facile solid phase synthesis strategy, and exhibited high fluorescence quantum yield. Cu (II) ions can be selectively adsorbed on the surface of the N-CNPs, and quench the fluorescence of N-CNPs with high efficiency. The fluorescence of N-CNPs/Cu(II) ions nanoprobes recovers in the presence of histidine, and can be applied for histidine detection with high sensitivity and excellent selectivity, as shown in Scheme 1. In addition, the N-CNP/Cu(II) ion nanoprobes show negligible cytotoxicity and superiority in resistance to photobleaching. The assay was successfully employed to the histidine determination in human serum and intracellular histidine imaging, which shows great promising in candidate for clinic diagnostic and drug screening.

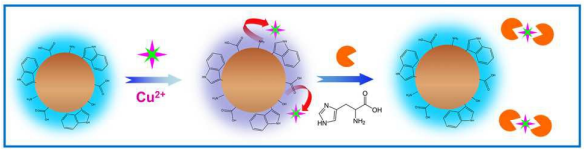

Scheme 1 Schematic illustration for fabricating Cu(II) ions modulated N-CNPs for fluorescence turn-on detection of histidine.

2. Materials and methods

2.1 Chemicals

Sodium alginate and all amino acids were purchased from Aladdin Chemistry Co. Ltd. (Shanghai, China). $CuCl_2$, $Fe(NO_3)_3$, $FeCl_2$, $Al(NO_3)_3$, $Co(NO_3)_2$, $Pb(NO_3)_2$, $ZnCl_2$, $AgNO_3$, $NiCl_2$, $CdCl_2$, $CrCl_3$, $CaCl_2$, $Hg(ClO_4)_2$ were bought from Beijing Chemical Reagent Co. Ltd. (Beijing, China). All reagents were of analytical grade and used as received without further purification. All solutions were prepared with double distilled water.

2.2 Apparatus and characterization

All fluorescence spectra were surveyed on an RF-5301PC fluorescence spectrophotometer (Shimadzu, Kyoto, Japan). The UV-vis spectra were obtained by a Hitachi U-3900 UV-vis spectrophotometer (Japan). The fluorescence images were acquired by a total internal reflection fluorescence microscope (TIRFM, Leica DM 4000B microscope).

2.3 Preparation of fluorescent N-CNPs

In a typical synthesis, 2.0 g of sodium alginate and 1.0 g of tryptophan were mixed in an agate mortar and ground to a uniform powder. Then the mixture was transferred into a 25 mL Teflon lined autoclave and heated at 220 °C for 6 h. The resultant brown mixture (yield ca. 62 %) was dissolved with ethanol. The brownish-yellow supernatant was collected by removing the large dots through centrifugation at 10 000 rpm for 10 min, and mixed with methylbenzene (ethanol/methylbenzene volume ratio was 1:3) and centrifuged at 14 000 rpm for 10 min. The precipitate was collected dried at 60 °C and a light brownish powder of N-CNPs was obtained.

2.4 Assays for histidine using the N-CNPs/Cu(II) ions ensemble

The N-CNPs/Cu(II) ions ensemble was prepared by diluting N-CNPs (10 μg/mL) and Cu(II) ions (30 μM) using phosphate buffered solution (PBS, 100 mM, pH6.0). For the detection of histidine, different concentrations of histidine were added to the N-CNPs/Cu(II) ions ensemble solution at room temperature. After that the fluorescence spectra of the mixture were recorded (excited at 270 nm). To investigate whether the other amino acids could interfere with the detection of histidine, the selectivity of the fluorescence assay was studied in detail. The concentration of all other amino acids was 75 μM in the solution containing 30 μM Cu(II) ions, and the same detection conditions were selected as mentioned above.

2.5 Cell culture and cell imaging

The HeLa cells were seeded in a 36-well plate and cultured in Dulbecco's modified Eagle's medium (DMEM) supplemented with 10 % fetal bovine serum (FBS), 2 mM glutamine, penicillin (100 units/mL), and streptomycin (100 units/mL) at 37 °C in a humidified atmosphere of 5 % CO_2 overnight. These cells were used in fluorescence imaging experimentation. In detailed procedures, the N-CNPs (0.1 mg mL^{-1}) were added to the cell culture, and the cells were incubated for another 6 h at 37 °C. For the Cu (II) ions treated samples, the cells were incubated with 0.1 mg mL^{-1} probe N-CNPs in DMEM for 6 h at 37 °C. After the removal of extracellular free probes by washing for three times, the cells were then incubated with 20 μM Cu (II) ions for 30 min at 37 °C. For the histidine treated samples, the cells were incubated with 0.1 mg mL^{-1} probe N-CNPs in DMEM for 6h at 37 °C. After the removal of extracellular free probes by washing for three times, the cells were then incubated with 20 μM Cu (II) ions for 30 min at 37 °C. The cells were washed twice with DMEM, and then 200 μM histidine was added and incubated for further 30 min. All the cells were washed with PBS for three times before observation under fluorescence microscopy in PBS.

3. Results and discussion

3.1 Characterization and optical properties of N-CNPs

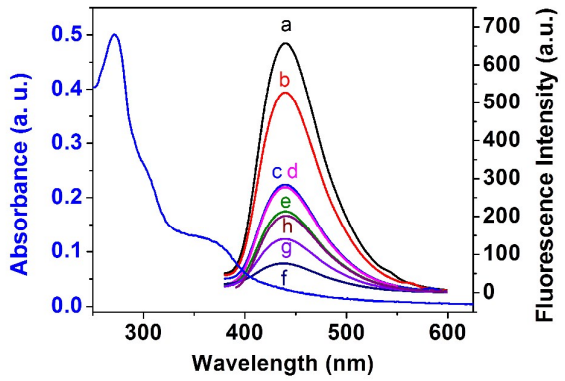

Fig. 1. UV-vis spectra and fluorescence emission spectra of the N-CNPs recorded at excitation wavelengths (curve a-h) of 270, 280, 290, 300, 310, 330, 350 and 370 nm.

The nitrogen-doped carbon nanoparticles (N-CNPs) synthesized by facial and solid phase method reported in our previous work[54] are monodispersed with near spherical morphology and exhibit an abundance of hydrophilic groups (Fig. S1, ESI†). The as-synthesized CNPs were further characterized by XPS. Three strong peaks at 532.0, 401.1, and 286.1 eV are observed in the XPS spectra (Fig. S2A, ESI†), which are attributed to O 1s, N 1s, and C 1s, respectively. The XPS spectrum of N 1s (Fig. S2B, ESI†) exhibits two fitted peaks at 398.5 and 399.5 eV, which are associated with nitrogen in a pyridine-like, pyrrolic-like nitrogen, respectively.[54] The N/C atomic ratio was calculated to be 4.05%. The facts demonstrated that the nitrogen atoms were doped as the form of pyridine-like nitrogen in the CNPs. The optical properties of N-CNPs were investigated using UV-vis and fluorescence spectroscopy. As shown in Fig. 1, the UV-vis spectra of the N-CNPs solution shows an absorption peak at ca. 270 nm, which is assigned to the π-π* transition of aromatic sp^2 domains.[55, 56] The absorption peak around 365 nm corresponds to the transition of n-π* transition of the C=O and C=N bond.[57, 58] The maximum emission wavelength of the N-CNPs is 440 nm when the N-CNPs are excited at 270 nm. The emission wavelength showed nearly no shift when the excitation wavelength is changed from 270 to 370 nm, indicating the uniformity of size and surface states.[59, 60] The constant emission wavelength indicated that the as prepared N-CNPs contained a single emitter only, which is favorable for the application of N-CNPs in quantitative assays and cell imaging. The fluorescence lifetime of the N-CNPs was measured by the time-correlated single photon (Fig. S3, ESI†) and the average lifetime of the N-CNPs is about 15.69 ns. By selecting quinine sulfate in sulfuric acid (0.1 mol L^{-1}) as the standard, the quantum yield of the N-CNPs is calculated to be 47.9 %, which is larger than those of N-CNPs reported in the literature.[43, 61, 62] Moreover, the cytotoxicity of N-CNPs was studied by the methylthiazol tetrazolium (MTT) assay, and the results indicate that the N-CNP possessed excellent biocompatibility (Fig. S4, ESI†). These results suggest that the N-CNPs has high quantum yield and excellent biocompatibility, which may be resulted from the plentiful hydrophilic groups on the surface of the as-synthesized N-CNPs, and is suitable for *in vivo* biomedical and imaging assay.

3.2 Fluorescence quenching of N-CNPs by Cu (II) ions

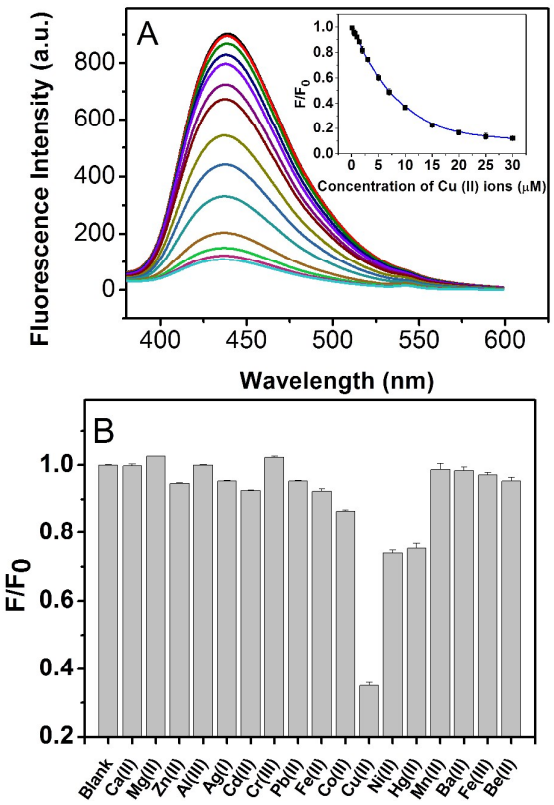

Fig. 2. (A) Fluorescence response of N-CNPs upon addition of various concentrations of copper ions (from top to bottom, 0, 0.05, 0.4, 0.6, 1, 3, 5, 7, 9, 15, 20, 25 and 30 μM) in a pH 6 PBS solution. Insert: plot of F/F_0 of N-CNPs *vs* the concentration of Cu (II) ions. (B) The influence of different metal ions on the fluorescence of N-CNPs. F_0 is the fluorescence intensity of N-CNPs and F is the fluorescence intensity of a mixture of metal ions, respectively.

When Cu(II) ions was added into the N-CNPs solution, the fluorescence of N-CNPs were quenched quickly, and the fluorescence intensity of the N-CNPs rapidly decreased as soon as the Cu (II) ions was added into the N-CNPs and kept stable during the following 30 min (Fig. S5, ESI†), indicating that the interaction between N-CNPs and Cu (II) ions reached equilibrium. As shown in Fig. 2A, the fluorescence intensity of the N-CNPs is sensitive to Cu (II) ions and decreases with increasing concentration of Cu (II) ions. The inset of Fig. 2A shows the relationship between the fluorescence intensity of N-CNPs and the concentration of Cu (II) ions, where the

fluorescence intensity decreases exponentially with the increasing concentration of Cu (II) ions. The fluorescence intensity of the N-CNPs decreased to about 10 % of the original fluorescence intensity after the addition of 30 μM Cu (II) ions, indicating that Cu (II) ions can effectively quench the fluorescence of N-CNPs, which can be ascribed to electron or energy transfer between Cu (II) ions and N-CNPs.[63, 64]

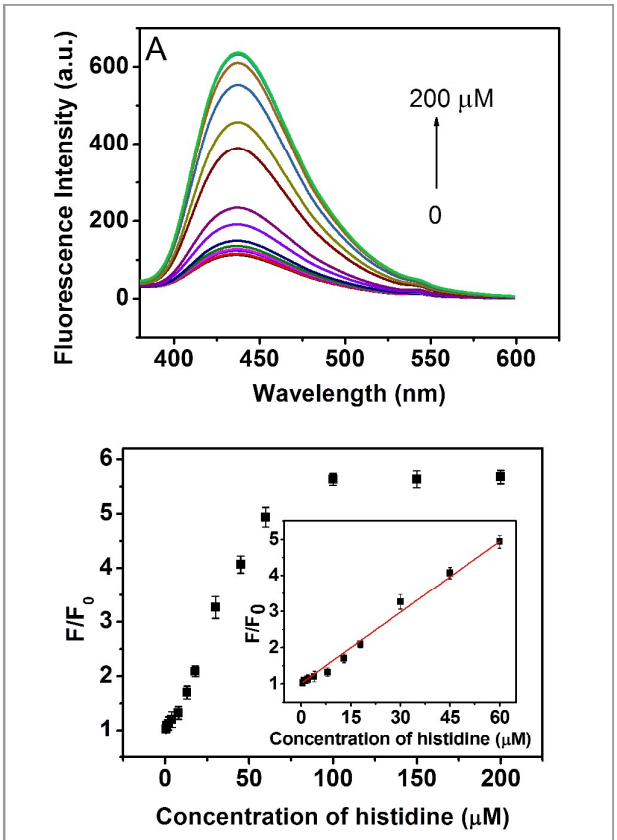

Fig. 3. (A) Fluorescence response of N-CNPs/Cu(II) ions aggregates upon addition of various concentrations of histidine (from bottom to top, 0, 0.5, 1, 2, 4, 8, 13, 18, 30, 45, 60, 80, 100,150 and 200 μM) in a pH 6 PBS solution. (B) Plot of F/F_0 of N-CNPs/Cu(II) ions vs the concentration of histidine.

Furthermore, the fluorescence responses of N-CNPs upon addition of different metal ions were also investigated. As shown in Fig. 2B, Cu (II) ions has the highest selectivity towards the fluorescence quenching of N-CNPs. The chelation of Cu (II) ions with amines of N-CNPs brought them into close proximity with each other, leading to substantial fluorescence quenching. To prove that the fluorescence quenching is related to the chelation of Cu (II) ions with amines, control experiments were done using CNPs. The corresponding CNPs were prepared in the same way but without tryptophan. It was found that the fluorescence intensity of CNPs cannot be strongly and selectively quenched by Cu (II) ions (Fig. S6, ESI†), proving that the formation of cupric amine plays an important role in the selective fluorescence response of the N-CNPs to the Cu (II) ions.

3.4 Fluorescence recovery of N-CNPs by histidine

The quenched fluorescence of the N-CNPs by Cu (II) ions can be basically recovered by adding histidine, and the fluorescence response nearly reached a plateau after 2 min and remained stable in the following 30 min at room temperature (Fig. S7, ESI†). This result indicates that the response of the N-CNPs/Cu(II) ions by histidine is rapid and stable, implying a promising application in a fast sensing of histidine without strict time control. UV-vis spectra were also applied to characterize the interactions after the addition of histidine. As shown in Fig. S8A ESI†, the absorption peak at 275 nm blue-shifted to 265 nm upon addition of Cu (II) ions in the histidine solution, probably could be attributed to the formation of a Cu-histidine complex. As shown in Fig. S8B ESI†, the addition of Cu (II) ions into the N-CNPs solution caused the absorption peak at 375 nm blue-shifted to 355 nm. Upon addition of histidine, the changed UV-vis spectra of the N-CNPs by Cu (II) ions can be basically recovered, which further demonstrated the effect of coordination between histidine and Cu (II) ions. This indicated that histidine competitively binds with Cu (II) ions in the N-CNPs/Cu(II) ions complex by forming a more stable complex Cu (II) ions/histidine. The interaction between Cu (II) ions and N-CNPs would be weakened by the competitive coordination of imidazole group, and part of Cu(II) ions could be taken away from the N-CNPs/Cu(II) ions complex,[65] then the fluorescence of N-CNPs would be dramatically enhanced.

In addition, the effect of the reaction pH values was also optimized, and the results revealed that the value of F_0/F in PBS buffer solution with pH 6.0 was higher than those of other pH values (Fig. S9, ESI†), so pH 6.0 was chosen for subsequent study. Moreover, control experiment without Cu (II) ions revealed that the fluorescence intensity of pure N-CNPs had a negligible change in the presence of histidine (Fig. S10, ESI†). This clearly suggested that the fluorescence enhancement of N-CNPs/Cu(II) ions solution was actually attributable to the formation of a more stable Cu (II) ions/histidine complex.

Fig. 3A shows the fluorescence responses of N-CNPs/Cu(II) ions nanoprobes upon addition of various concentrations of histidine under the optimal experimental conditions. The fluorescence intensity gradually restored with the increasing concentration of histidine and reached a platform after 100 μM. As shown in Fig. 3B, a linear relationship between the fluorescence intensity enhancement and the concentration of histidine was obtained in the range from 0.5 μM to 60 μM with a detection limit of 150 nM (S/N = 3). The linear regression equation was $F/F_0 = 0.0681c$ (μM) + 0.9503, r = 0.997 (F_0 and F are the fluorescence intensities at 440 nm in the absence and presence of histidine, respectively). Compared with those reported strategies for histidine detection (Table S1, ESI†), our developed method has the advantages including no chemical modification, high sensitivity, low detection limit and relatively wide detection range, which shows great promising in biomedical and intracellular imaging assay.

The fluorescence responses of N-CNPs/Cu(II) ions were also investigated in the presence of various amino acids. The results indicated that the tested amino acids have less influence on the histidine determination by using the N-CNPs/Cu(II) ions as nanoprobes (Fig. 4). It was noted that the fluorescence of N-CNPs/Cu(II) ions nanoprobes recovered initially by the addition of cysteine, and then it quenched in 10 min (Fig. S11, ESI†). The detection of histidine is more suitable in the CNPs/Cu (II) ions system because the imidazole side-chain moiety contained in histidine plays an important role in dissociating Cu (II) ions from the surface of N-CNPs.[30] This fact demonstrated that the as designed biosensor possessed excellent selectivity toward histidine determination.

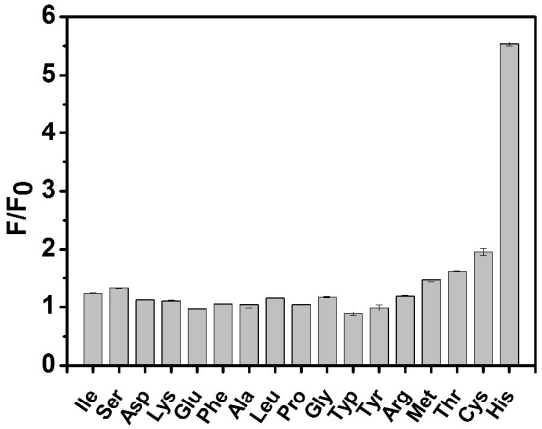

Fig. 4. Fluorescence response of N-CNPs/Cu(II) ions in the presence of 75 μM various amino acid.

3.3 Application of N-CNPs/Cu(II) ions in human serum and living cells

The detection of histidine in human serum samples was carried out to evaluate the feasibility of the proposed method in real sample detection. The results are shown in Table 1. The relative standard deviation (RSD) was lower than 3.9 and the recoveries were between 96.8 % and 103.6 %. These results demonstrated the potential applicability of the N-CNPs/Cu(II) ions based turn-on fluorescence probe for the detection of histidine in human serum samples.

Table 1 Measurement results of histidine in human serum samples, n = 5. The original concentrations of histidine in human serum samples were subjected to a 50-fold dilution with PBS.

No.	Added (μM)	Found (μM)	Recovery (%)	RSD (%)
1	10.00	10.14	103.6	2.3
2	20.00	19.63	98.2	2.8
3	30.00	29.03	96.8	3.9

In addition, the intracellular imaging of histidine using N-CNPs/Cu(II) ions complex as nanoprobes was explored. Before the experiments, the cytotoxicity of the N-CNPs/Cu(II) ions complex nanoprobes was studied by the MTT assay. It was observed that the viability of the cells remained unchanged when the concentration of N-CNPs/Cu(II) ions nanoprobes was as high as 500 μg mL^{-1} (Fig. 5). The result suggests that the N-CNPs/Cu(II) ions nanoprobe has excellent biocompatibility, and can be effectively applied for *in vivo* cell imaging and biological labeling. Fig. 6 shows TIRFM images of HeLa cells. When the N-CNPs probe (10 μM) was loaded into the HeLa cell medium, strong blue fluorescence was observed (Fig. 6A). This suggests that the N-CNPs has good cell permeability and is suitable for live cell imaging. After incubating with 20 μM Cu (II) ions for another 30 min, a remarkable fluorescence decrease was observed (Fig. 6B). While further treatment of the cells with 200 μM histidine for 30 min recovers the fluorescence signal (Fig. 6C). In addition, there is no reduction in fluorescence intensity even after excitation for a prolonged time. These results implicated the potential ability of N-CNPs/Cu(II) ions to monitor histidine levels in living cells.

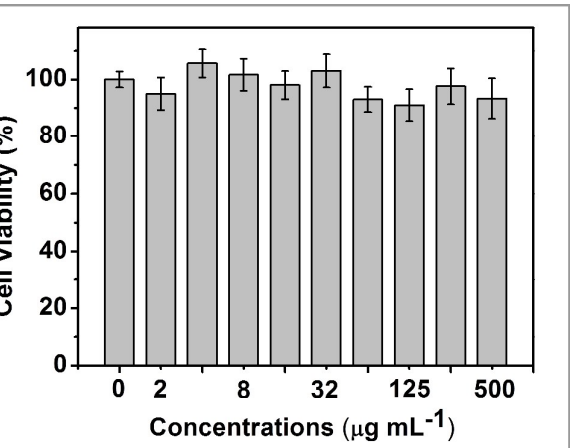

Fig. 5. Cell viability after incubation with N-CNPs/Cu (II) ions for 24 h.

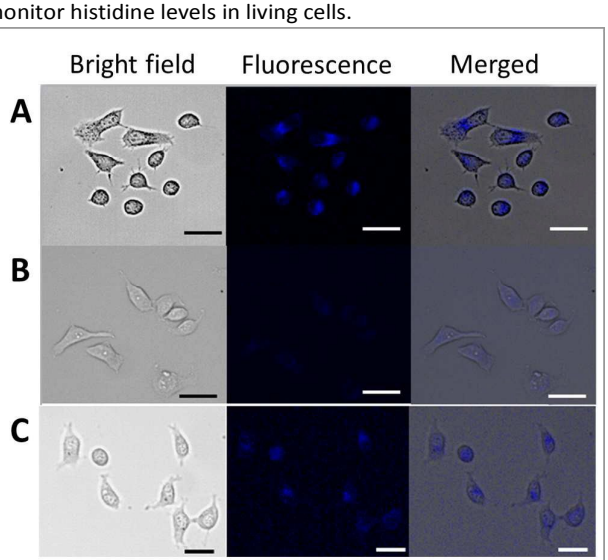

Fig. 6. TIRFM images of HeLa cells excited at 365 nm. (A) Stained with N-CNPs, (B) stained with N-CNPs and Cu (II) ions, (C) stained with N-CNPs/Cu(II) ions, and histidine. Scale bar: 20 μm.

4. Conclusions

In conclusion, we have developed a rapid, sensitive, and specific fluorescence turn-on assay for the detection of histidine *in vitro* and in living cells. The mechanism of the turn-on detection of histidine was based on the histidine being able to effectively shelter the quenching due to the binding of Cu (II) ions and its imidazole group, which removes Cu (II) ions from the surface of N-CNPs. The developed fluorescent sensor offered high selectivity for histidine over other amino acids and sensitivity with a low limit of detection (150 nM). Furthermore, the fluorescent sensor could be readily applied to the rapid and sensitive histidine detection in human serum and living cell, exhibiting great opportunities for practical application in biological and clinical diagnosis fields.

Acknowledgements

This work was financially supported by the National Natural Science Foundation of China (No. 21375073, No. 21235004), and Tsinghua University Initiative Scientific Research Program (2014z21027).

Notes and references

1 Y. Hu, Q. Wang, C. Zheng, L. Wu, X. Hou and Y. Lv, *Anal. Chem.*, 2014, **86**, 842-848.
2 M. R. Ross, A. M. White, F. Yu, J. T. King and K. J. Kubarych, *J. Am. Chem. Soc.*, 2015, **137**, 10164-10176.
3 J. Elferich, D. M. Williamson, L. L. David and U. Shinde, *Anal. Chem.*, 2015, **87**, 7909-7917.
4 D. L. Ma, W. L. Wong, W. H. Chung, F. Y. Chan, P. K. So, T. S. Lai, Z. Y. Zhou, Y. C. Leung and K. Y. Wong, *Angew. Chem.; Int. Ed.*, 2008, **47**, 3735-3739.
5 S. Qiu, M. Miao, T. Wang, Z. Lin, L. Guo, B. Qiu and G. Chen, *Biosens. Bioelectron.*, 2013, **42**, 332-336.
6 S. Seshadri, A. Beiser, J. Selhub, P. F. Jacques, I. H. Rosenberg, R. B. D'Agostino, P. W. F. Wilson and P. A. Wolf, *New Engl. J. Med.*, 2002, **346**, 476-483.
7 M. Watanabe, M. E. Suliman, A. R. Qureshi, E. Garcia-Lopez, P. Barany, O. Heimburger, P. Stenvinkel and B. Lindholm, *Am. J. Clin. Nutr.*, 2008, **87**, 1860-1866.
8 N. Tateda, K. Matsuhisa, K. Hasebe, N. Kitajima and T. Miura, *J. Chromatogr. B*, 1998, **718**, 235-241.
9 J. Meng, W. Zhang, C.-X. Cao, L.-Y. Fan, J. Wu and Q.-L. Wang, *Analyst*, 2010, **135**, 1592-1599.
10 J. Nai, Z. Chen, H. Li, F. Li, Y. Bai, L. Li and L. Guo, *Chem. Eur. J.*, 2013, **19**, 500-507.
11 Z. Chen, J. Nai, H. Ma and Z. Li, *Electrochim. Acta*, 2014, **116**, 258-262.
12 D. R. Bae, W. S. Han, J. M. Lim, S. Kang, J. Y. Lee, D. Kang and J. H. Jung, *Langmuir*, 2010, **26**, 2181-2185.
13 S. Zhang, C. Yang, W. Zhu, B. Zeng, Y. Yang, Y. Xu and X. Qian, *Org. Biomol. Chem.*, 2012, **10**, 1653-1658.
14 M. A. Hortala, L. Fabbrizzi, N. Marcotte, F. Stomeo and A. Taglietti, *J. Am. Chem. Soc.*, 2003, **125**, 20-21.
15 X. Zheng, T. Yao, Y. Zhu and S. Shi, *Biosens. Bioelectron.*, 2015, **66**, 103-108.
16 T. Egawa, K. Hirabayashi, Y. Koide, C. Kobayashi, N. Takahashi, T. Mineno, T. Terai, T. Ueno, T. Komatsu, Y. Ikegaya, N. Matsuki, T. Nagano and K. Hanaoka, *Angew. Chem.; Int. Ed.*, 2013, **52**, 3874-3877.
17 X. Gao, C. Ding, A. Zhu and Y. Tian, *Anal. Chem.*, 2014, **86**, 7071-7078.
18 Y. Wang, L. Tang, Z. Li, Y. Lin and J. Li, *Nat. Protoc.*, 2014, **9**, 1944-1955.
19 R. Deng, L. Tang, Q. Tian, Y. Wang, L. Lin and J. Li, *Angew. Chem.; Int. Ed.*, 2014, **53**, 2389-2393.
20 U. G. Reddy, H. Agarwalla, N. Taye, S. Ghorai, S. Chattopadhyay and A. Das, *Chem. Commun.*, 2014, **50**, 9899-9902.
21 X. Wang, Q. Miao, T. Song, Q. Yuan, J. Gao and G. Liang, *Analyst*, 2014, **139**, 3360-3364.
22 F. Pu, Z. Huang, J. Ren and X. Qu, *Anal. Chem.*, 2010, **82**, 8211-8216.
23 T. Chen, L. Yin, C. Huang, Y. Qin, W. Zhu, Y. Xu and X. Qian, *Biosens. Bioelectron.*, 2015, **66**, 259-265.
24 J. Li, X. Hong, D. Li, K. Zhao, L. Wang, H. Z. Wang, Z. L. Du, J. H. Li, Y. B. Bai and T. J. Li, *Chem. Commun.*, 2004, 1740-1741.
25 Y. Wang, K. Qu, L. Tang, Z. Li, E. Moore, X. Zeng, Y. Liu and J. Li, *TrAC-Trend. Anal. Chem.*, 2014, **58**, 54-70.
26 H. Feng, R. Cheng, X. Zhao, X. Duan and J. Li, *Nat. Commun.*, 2013, **4**. 1539-1539.
27 L. Tang, H. Feng, J. Cheng and J. Li, *Chem. Commun.*, 2010, **46**, 5882-5884.
28 W. Bian, F. Wang, Y. Wei, L. Wang, Q. Liu, W. Dong, S. Shuang and M. M. Choi, *Anal. Chim. Acta.*, 2015, **856**, 82-89.
29 S. Liu, F. Shi, L. Chen and X. Su, *Analyst*, 2013, **138**, 5819-5825.
30 F. Shi, S. Liu and X. Su, *Talanta*, 2014, **125**, 221-226.
31 Y. Zhou, T. Zhou, M. Zhang and G. Shi, *Analyst*, 2014, **139**, 3122-3126.
32 Y. He, X. Wang, J. Zhu, S. Zhong and G. Song, *Analyst*, 2012, **137**, 4005-4009.
33 M. Shamsipur, F. Molaabasi, M. Shanehsaz and A. A. Moosavi-Movahedi, *Microchim. Acta*, 2015, **182**, 1131-1141.
34 W. Zhou, L. Lin, W. Wei, H. Jin, J. Li and L. Guo, *Rsc Adv.*, 2013, **3**, 7933-7937.
35 L. H. Tang, H. B. Feng, J. S. Cheng and J. H. Li, *Chem. Commun.*, 2010, **46**, 5882-5884.
36 J. Sun, F. Yang, D. Zhao, C. Chen and X. Yang, *ACS Appl. Mater. Interfaces*, 2015, **7**, 6860-6866.
37 C. Ding, A. Zhu and Y. Tian, *Acc. Chem. Res.*, 2014, **47**, 20-30.
38 P. Innocenzi, L. Malfatti and D. Carboni, *Nanoscale*, 2015, **7**, 12759-12772.
39 X. T. Zheng, A. Ananthanarayanan, K. Q. Luo and P. Chen, *Small*, 2015, **11**, 1620-1636.
40 L. Lin, Y. Liu, X. Zhao and J. H. Li, *Anal. Chem.*, 2011, **83**, 8396-8402.

41 H. Huang, C. Li, S. Zhu, H. Wang, C. Chen, Z Wang, T. Bai, Z. Shi and S. Feng, *Langmuir*, 2014, **30**, 13542−13548.
42 Y. Dong, R. Wang, G. Li, C. Chen, Y. Chi and G. Chen, *Anal. Chem.*, 2012, **84**, 6220-6224.
43 H. Zhang, Y. Chen, M. Liang, L. Xu, S. Qi, H. Chen and X. Chen, *Anal. Chem.*, 2014, **86**, 9846-9852.
44 P. Shen and Y. Xia, *Anal. Chem.*, 2014, **86**, 5323-5329.
45 J. Zong, X. Yang, A. Trinchi, S. Hardin, I. Cole, Y. Zhu, C. Li, T. Muster and G. Wei, *Biosens. Bioelectron.*, 2014, **51**, 330-335.
46 A. Zhu, Q. Qu, X. Shao, B. Kong and Y. Tian, *Angew. Chem.; Int. Ed.*, 2012, **51**, 7185-7189.
47 W. Shi, X. Li and H. Ma, *Angew. Chem.; Int. Ed.*, 2012, **51**, 6432-6435.
48 J. Xu, F. Zeng, H. Wu, C. Hu, C. Yu and S. Wu, *Small*, 2014, **10**, 3750-3760.
49 L. Wang and H. S. Zhou, *Anal. Chem.*, 2014, **86**, 8902-8905.
50 S. Liu, N. Zhao, Z. Cheng and H. Liu, *Nanoscale*, 2015, **7**, 6836-6842.
51 J. Hou, F. Zhang, X. Yan, L. Wang, J. Yan, H. Ding and L. Ding, *Anal. Chim. Acta*, 2015, **859**, 72-78.
52 Z. Li, H. Yu, T. Bian, Y. Zhao, C. Zhou, L. Shang, Y. Liu, L.-Z. Wu, C.-H. Tung and T. Zhang, *J. Mater. Chem. C*, 2015, **3**, 1922-1928.
53 H. Ding, J.-S. Wei and H.-M. Xiang, *Nanoscale*, 2014, **6**, 13817-13823.
54 X. Zhu, T. Zhao, Z. Nie, Y. Liu and S. Yao, *Anal. Chem.*, 2015, **87**, 8524-8530.
55 Y. Li, Y. Zhao, H. Cheng, Y. Hu, G. Shi, L. Dai and L. Qu, *J. Am. Chem. Soc.*, 2012, **134**, 15-18.
56 X. Zhu, X. Zuo, R. Hu, X. Xiao, Y. Liang and J. Nan, *Mater. Chem. Phy.*, 2014, **147**, 963-967.
57 Y. Dong, H. Pang, H. B. Yang, C. Guo, J. Shao, Y. Chi, C. M. Li and T. Yu, *Angew. Chem.; Int. Ed.*, 2013, **52**, 7800-7804.
58 M. Zheng, Z. Xie, D. Qu, D. Li, P. Du, X. Jing and Z. Sun, *ACS Appl. Mater. Interfaces*, 2013, **5**, 13242-13247.
59 Q.-L. Zhao, Z.-L. Zhang, B.-H. Huang, J. Peng, M. Zhang and D.-W. Pang, *Chem. Commun.*, 2008, 5116-5118.
60 X. Zhu, X. Xiao, X. Zuo, Y. Liang and J. Nan, *Part. Part. Syst. Charact.*, 2014, **31**, 801-809.
61 Y. Yang, J. Cui, M. Zheng, C. Hu, S. Tan, Y. Xiao, Q. Yang and Y. Liu, *Chem. Commun.*, 2012, **48**, 380-382.
62 Q. Liang, W. Ma, Y. Shi, Z. Li and X. Yang, *Carbon*, 2013, **60**, 421-428.
63 A. Salinas-Castillo, M. Ariza-Avidad, C. Pritz, M. Camprubi-Robles, B. Fernandez, M. J. Ruedas-Rama, A. Megia-Fernandez, A. Lapresta-Fernandez, F. Santoyo-Gonzalez, A. Schrott-Fischer and L. F. Capitan-Vallvey, *Chem. Commun.*, 2013, **49**, 1103-1105.
64 C. Hu, C. Yu, M. Li, X. Wang, J. Yang, Z. Zhao, A. Eychmueller, Y. P. Sun and J. Qiu, *Small*, 2014, **10**, 4926-4933.
65 J. F. Folmer-Andersen, V. M. Lynch and E. V. Anslyn, *Chem. Eur. J.*, 2005, **11**, 5319-5326.